

PatchProto Networks for Few-shot Visual Anomaly Classification

Jian Wang^a, Yue Zhuo^{a,*}

^a*College of Control Science and Engineering, Zhejiang University*

Abstract

The visual anomaly diagnosis can automatically analyze the defective products, which has been widely applied in industrial quality inspection. The anomaly classification can classify the defective products into different categories. However, the anomaly samples are hard to access in practice, which impedes the training of canonical machine learning models. This paper studies a practical issue that anomaly samples for training are extremely scarce, i.e., few-shot learning (FSL). Utilizing the sufficient normal samples, we propose PatchProto networks for few-shot anomaly classification. Different from classical FSL methods, PatchProto networks only extract CNN features of defective regions of interest, which serves as the prototypes for few-shot learning. Compared with basic few-shot classifier, the experiment results on MVTec-AD dataset show PatchProto networks significantly improve the few-shot anomaly classification accuracy.

Keywords: Few-shot learning, anomaly classification, anomaly segmentation

1. Introduction

The anomaly diagnosis based on computer-vision techniques can automatically analyze the defective samples, including tasks like anomaly detection, segmentation and classification. Anomaly detection [14, 12] has been a prevalent research topic recently, which aims to identify the unusual patterns (i.e., outliers) that deviate from the normal observations. Anomaly segmentation [24, 18] highlights the anomaly variables (e.g., pixels) in input space, which provides the explanation for the detection results. Furthermore, anomaly classification seeks to recognize what types the anomaly samples belong to, which could benefit the maintenance of the industrial systems.

The major impediment of anomaly classification is the scarcity of anomaly samples. This issue recently has been an active research area in the field of machine learning, also known as few-shot learning (FSL). FSL classifies new data with only a few training samples¹ with supervised information. Anomaly classification is a typical example of FSL, since the defective samples rarely occur and are hard to collect. In past few years, many FSL approaches

*Corresponding author

Email addresses: wangjianxxx818@gmail.com (Jian Wang), zhuoy1995@zju.edu.cn (Yue Zhuo)

¹When there is only one training sample of each class, the problem becomes one-shot learning.

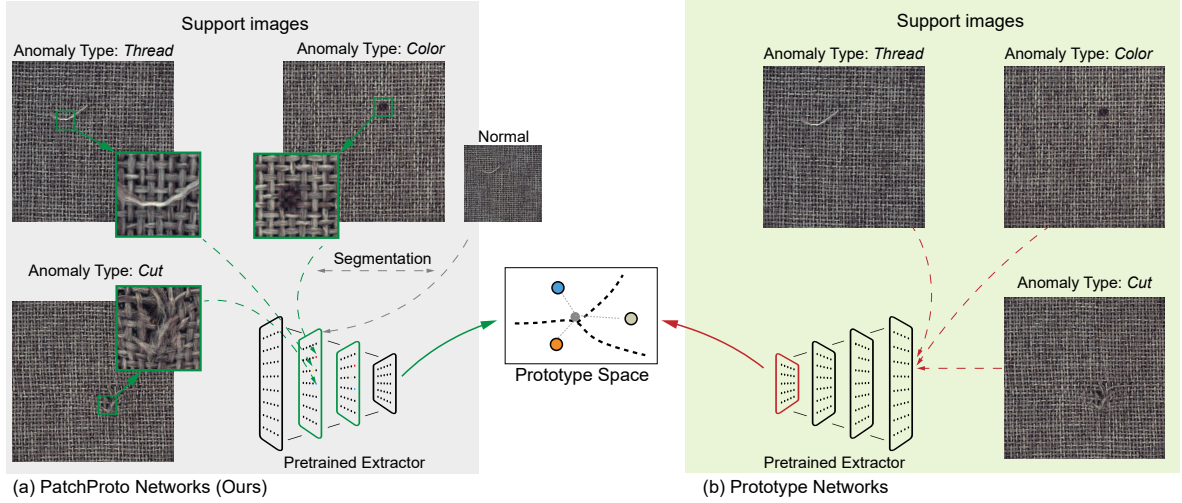


Figure 1: **Comparison between (a) PatchProto and (b) Prototype networks** for textile anomaly classification in MVTec-AD dataset [2].

are proposed, including classical models like Model-Agnostic Meta-Learning (MAML) [8], Matching Networks [21], and Prototypical Networks [20].

Industrial anomaly classification is a little different. Unlike the universal FSL benchmarks (e.g., Omniglot [19] and CUB [22]) consisting of hundreds of class labels, the number of industrial anomaly type is relatively small, thus it is commonly infeasible to apply meta-training in FSL anomaly classification. Fortunately, industrial datasets contains a large number of normal samples, which can be utilized for classifying the anomaly samples.

Inspired by the anomaly detection methods, this study first locates the anomaly regions using normal samples, and then extracts CNN embeddings of the anomaly regions. During the test phase, we compute the anomaly embedding distances between query and support sets to identify the class label of query samples. Fig. 1 compares our proposal and Prototype networks. PatchProto networks adapt the core idea of Prototype networks, one of the canonical FSL methods. Distinctively, PatchProto networks compute the prototypes in the shallow layers rather than bottleneck feature and only the embeddings of anomaly pixels (i.e., patches) are concerned. The anomaly patches are located by contrasting with normal samples, which has been widely applied in the anomaly segmentation works [15, 7, 5].

In summary, we propose PatchProto networks as an effective FSL anomaly classification method, by (1) using the CNN feature embeddings of only anomaly patches to serve as the prototypes, (2) extracting features from the shallow layers. The anomaly segmentation work [15] has shown that using mid-level pertained network features can reduce the biases towards ImageNet classes. In the following sections, this paper will discuss the significance of forcing model to focus on the anomaly patches. On 14 sub-datasets of MVTec-AD, PatchProto networks achieves 16% and 10% higher average accuracy over vanilla Prototype networks and the simple combining Prototype networks with anomaly segmentation (Prototype + segmentation).

2. Background and related works

2.1. Anomaly diagnosis

Many anomaly diagnosis methods ensemble both detection and segmentation facility. Most approaches learn the representations of normal data in a unsupervised manner, for which many generative models are utilized, such as GANs [6], (Variational) AutoEncoders [25, 1] and flow models [16]. During the test phase, the representations of novel samples are inferred and the anomaly detection results are computed by the reconstruction errors or KNN methods. For these methods, anomaly segmentation can be subsequently achieved by pixel-level reconstruction errors or some feature attribution methods.

Recently, some research shows that, with the help of models pretrained on large external datasets (e.g., ImageNet), the performance of industrial anomaly detection can be further improved. Approaches like SPADE [5], PaDiM [7] and PatchCore [15] extract the image features with pretrained networks at patch-level, then use similarity measures to score the patch-level abnormality. Among them, PatchCore achieved state-of-the-art on total recall perform of both detection and segmentation.

Anomaly classification is a further task that identifies the types of anomaly samples, which provides more detailed information than anomaly detection. Data scarcity is always the major issue in the anomaly classification. Natarajan et al. [13] propose voting-based methods to solve the over-fitting caused by small textile datasets. There are many works presented for the few-shot industrial fault classification, in the field like rolling bearing [11], chemical process [26], and power systems [10].

2.2. Few-shot learning

FSL is a task of classification, in which the sample numbers are quite small (typically less than 10 each class). In FSL setting, the labeled dataset for training is named as support set and the samples with unknown labels for testing compose the query set. A few-shot classification model uses the information from the support set to classify the query images. Given support set with N different class labels and K samples each class, the FSL is named N -way K -shots problem.

FSL is more challenging than other problems like semi-supervised or imbalanced classification, since the extremely scarce samples would easily lead to over-fitting and bad performance on test sets. The popular FSL solutions are based on meta-learning [8], which first learn from the relevant classes of abundant samples and then transfer to minor classes.

However, the meta-learning is not suitable for anomaly classification, since there is not enough relevant classes for pre-training. This paper focuses on another prevalent FSL strategy, metric learning. Its core idea is to compute the embeddings of input and use similarity metrics of embeddings to classify samples. Prototypical Networks [20] is a typical approach. It uses a pretrained CNN to project support and query samples into the feature space, and computes the prototype for each class by averaging the embeddings of support samples. For query samples, they are classified by the distances from their embeddings to each prototype.

For visual anomaly diagnosis, the few-shot learning is more studied in anomaly detection. Visual Anomaly and Novelty Detection (VAND) 2023 Challenge proposes two tracks of

Algorithm 1 PatchProto networks

Input: ϕ : Pretrained CNN for embedding extraction \mathcal{X}_N : normal samples
 $\{(\mathcal{X}_S, \mathcal{Y}_S)\}$: support set
 \mathcal{X}_Q : query set
1: $\mathcal{Z}_N, \mathcal{Z}_S, \mathcal{Z}_Q = \phi(\mathcal{X}_N), \phi(\mathcal{X}_S), \phi(\mathcal{X}_Q) \triangleleft$ extract embeddings
2: $s_{\mathcal{Z}_S}, s_{\mathcal{Z}_Q} = f_s(\mathcal{Z}_S, \mathcal{Z}_N), f_s(\mathcal{Z}_Q, \mathcal{Z}_N) \triangleleft$ compute patch-level anomaly score
3: $\mathcal{Z}_S^P, \mathcal{Z}_Q^P = f_p(\mathcal{Z}_S, s_{\mathcal{Z}_S}), f_p(\mathcal{Z}_Q, s_{\mathcal{Z}_Q}) \triangleleft$ select anomaly embeddings
4: $\mathcal{Z}^y = \{z^i | z^i \in \mathcal{Z}_S^P, i = y \in \mathcal{Y}\} \triangleleft$ gather prototypes of each class
5: $d^y = D(\mathcal{Z}_Q^P, \mathcal{Z}^y), y \in \mathcal{Y} \triangleleft$ measure distances to prototypes
Output: $\mathcal{Y}_Q = \{y | y = \arg \min d^y\}$ Predicted labels of query set

zero-shot and few-shot anomaly detection. Given the limited number of normal samples, April-GAN [4] and an optimized PatchCore [17] achieve the best performances on detecting anomaly samples. However, the scenario that the anomaly samples are scarce (i.e., few-shot visual anomaly classification), is less concerned, while we believe this setting is more practical.

3. Method

This section present our proposal for few-shot visual anomaly classification, PatchProto networks. It consists of two major parts: anomaly prototypes and distance measures, which will be introduced in sequence. Algorithm 1 presents the pseudo code of PatchProto networks.

3.1. Anomaly prototypes

Unlike typical Prototype networks that use flattened bottleneck embeddings as the prototypes, PatchProto networks select partial mid-level embeddings that are closely related to the anomaly regions of input images. We first determine the anomaly scores of image patches by the embeddings distances to the normal samples. Specifically, we adapt scoring algorithm (f_s in Algorithm 1) of PatchCore² that achieves state-of-the-art anomaly segmentation performance.

In anomaly classification, the normal image pixels do not contain positive information to distinguish different anomaly types, and only the anomaly regions determine the image types. Hence, we need to select the embeddings that most likely correspond to the anomaly image regions. Given the embeddings \mathcal{Z}_S with anomaly scores $s_{\mathcal{Z}_S}$, one direct approach is to select the top- k embeddings with highest scores (k is a fixed number). However, the size of anomaly region in each image is different, so a fixed embedding number is imprecise. A

²The anomaly scoring is not limited to one algorithm, and any pixel-wise anomaly segmentation algorithm can be applied.

Algorithm 2 Anomaly embedding selection (taking one image as example)

Input: $z \in \mathcal{Z}$: embeddings of one image $s \in s_{\mathcal{Z}}$: anomaly scores of embeddings

γ : threshold

m : embedding number upper bound

1: $z^* = \{\}$, $c = 0, i = 0$

2: $s = softmax(s) \triangleleft$ normalization

3: Index the elements of z_s and s by s in decreasing order

4: **while** $c < \gamma$ and $|z^*| < m$ **do**

5: $z^* = z^* \cup z[i]$

6: $c += s[i]$

7: $i += 1$

8: **end while**

Output: $z^* = \{\}$ Selected anomaly embeddings

feasible way is to select the embeddings that contribute a certain percentage (γ) of the total score, just like the way to select PCA eigenvectors. This approach can adaptively select the most abnormal embeddings of the input images. Nevertheless, if the image anomaly region cannot be precisely located, this approach will collapse and select a very large anomaly region, which is totally misleading. To avoid this, we set a upper bound (m) for the anomaly patch number. Algorithm 2 shows the procedure for selecting the anomaly embeddings (f_p in Algorithm 1).

The anomaly embeddings of support and query sets are selected by the same algorithm. For support set, we simply gather the embeddings of identical anomaly type to get the prototypes \mathcal{Z}^y . Since the embedding sizes of support samples are not fixed, we do not take the mean of embeddings as the prototype, which is commonly applied in the other prototype-based methods.

3.2. Distance measures

Given the anomaly embeddings of support and query sets, the query samples can be classified by measuring the distances between its embeddings to the prototypes. A prototype contains a set of embeddings, so the aim is to measure the distance between two vector sets. Given a query anomaly embeddings $z_Q \in \mathcal{Z}_Q$, the distance of each single query embedding $z_Q^{(i)}$ is measured by the maximal Cosine distance w.r.t. different prototype embeddings $\mathcal{Z}^y[n]$. The distance measure of a single query sample is obtained by summation with the weights of normalized anomaly scores $s_{z_Q^{(i)}}$. Finally, we gain the class distance by the mean distance over (N) different prototype embeddings of the same class:

$$d^y = \frac{1}{N} \sum_{n=0}^N \sum_{i=0}^{|z_Q|} s_{z_Q^{(i)}} \times \min[1 - \text{Cos}(z_Q^{(i)}, \mathcal{Z}^y[n])] \quad (1)$$

Table 1: Few-shot classification accuracy on MVTec-AD dataset (averaged over subsets) (%)

	1-shot	3-shot	5-shot
Matching networks [9]	39.0	42.4	46.0
SimpleShot [23]	39.6	48.1	53.9
FineTune [3]	39.6	48.3	54.0
Prototype networks [20]	38.3	49.1	53.7
Segmentation* + Proto	44.2	54.2	57.6
PatchProto networks (Ours)	57.9	65.5	68.9

* Anomaly segmentation by PatchCore.

Based on the class distances, we can easily predict label of query samples by selecting the closest class.

4. Experiments

4.1. Details

The experiment is performed on the MVTec Anomaly Detection dataset. We use 14 of 15 sub-datasets³. Each sub-dataset contains at least 200 normal samples, of which each anomaly class contains 10 to 20 samples. In experiments, we only classify anomaly samples while normal samples are not considered. We resize the images to the size of 224×224 and do not apply any augmentation techniques. We use WideResNet-50-2 pretrained on ImageNet as the feature extractor, also applied for other compared methods.

4.2. Results

Table 1 reports the average few-shot classification accuracy on MVTec-AD, which compares networks with typical FSL methods including Matching networks [9], SimpleShot [23], FineTune [3] and Prototype networks [20]. Given the original anomaly images as the input, typical FSL classifiers achieve similar accuracy. When preprocessing anomaly images by segmentation, few-shot accuracy cloud be significantly improved (Segmentation + Proto). This validates that excluding irrelative image regions can effectively benefit the anomaly classification.

Our proposal, PatchProto networks, achieve the best few-shot classification accuracy over these methods, which is about 15% higher than FSL methods with original input and 10% higher than segmentation input. Intriguingly, the advantage of PatchProto networks is especially significant on 1-shot, which we believe is mainly attributed to the anomaly embedding used for prototypes.

³The dataset “toothbrush” only has one anomaly type, which is excluded.

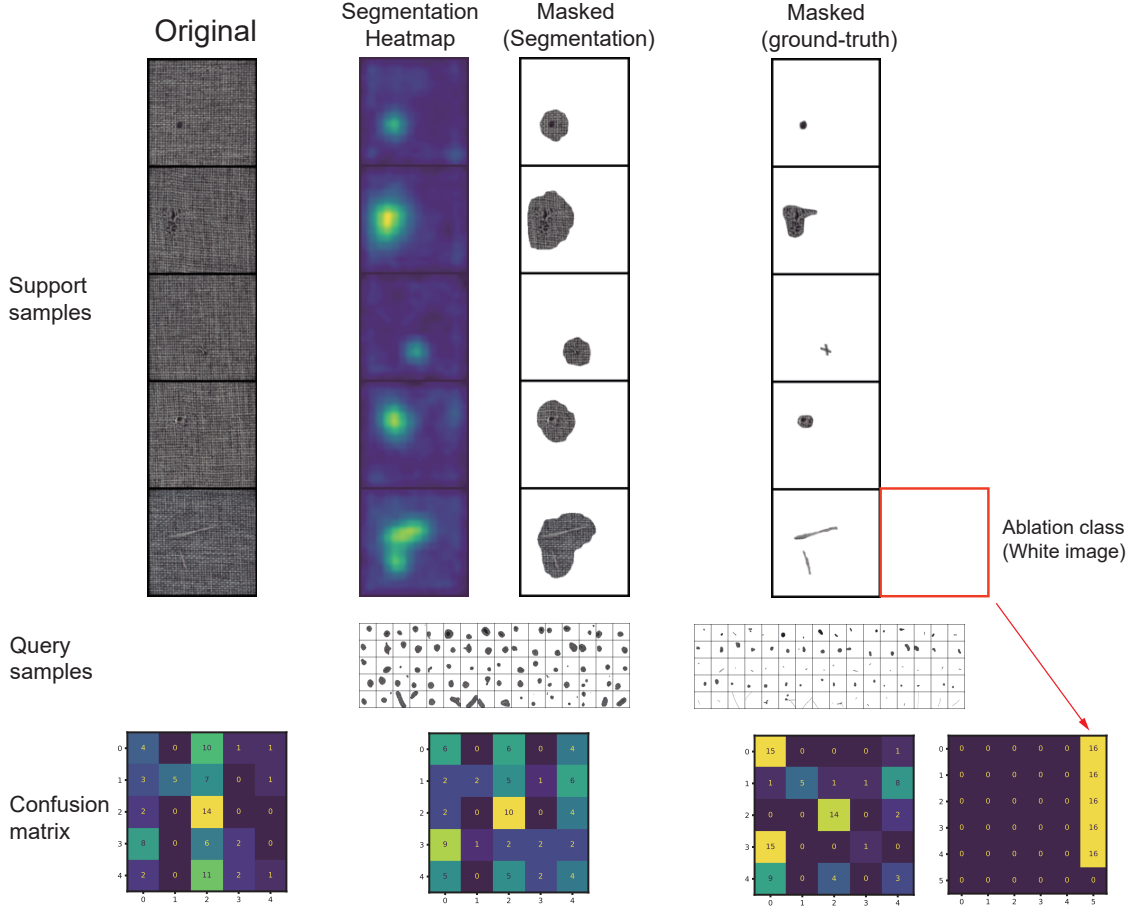


Figure 2: **Illustration of baselines for ablation study.**

4.3. Ablation study

It is straightforward to compare our proposal with the Prototype networks. As baselines, we process support and query sets in three different ways: (1) the original images; (2) the images masked by the PatchCore anomaly segmentation; (3) the images masked by the manually annotated (ground-truth) segmentation. Figure 2 shows the baselines for ablation study, where the “carpet” subset of MVTec-AD are displayed and each anomaly class has one single support samples.

For original anomaly samples, the confusion matrix of Prototype networks shows that model tends to classify samples into class “2” label. This is mainly due to the large normal pixels in the class “2” support image. Since the normal pixels take up the main body of the anomaly image and anomaly region is only a small part, it is natural for models to predict that inputs are more similar to the images that are close to normal samples (e.g., class “2” support image in Figure 2).

Preprocessing images with anomaly segmentation can avoid this problem, shown in the middle of Figure 2. Prototype networks with masked anomaly images have higher accuracy.

Table 2: Few-shot classification accuracy on different subsets of MVTec-AD dataset (%)

	PatchProto networks			Masked (Segmentation)			Masked (Ground-truth)		
	1-shot	3-shot	5-shot	1-shot	3-shot	5-shot	1-shot	3-shot	5-shot
bottle	52.2	52.0	57.5	61.8	69.8	72.9	73.0	76.5	77.8
cable	62.5	69.7	73.0	44.4	59.6	64.0	60.8	71.1	71.5
capsule	34.5	37.9	42.9	31.4	37.6	40.3	37.7	42.8	46.1
carpet	56.6	67.7	73.0	33.8	59.4	60.7	45.7	58.9	69.7
grid	40.6	38.7	43.2	36.0	50.0	48.0	44.4	53.0	62.7
hazelnut	81.0	95.3	93.7	50.9	67.1	77.5	70.0	82.9	83.3
leather	71.9	84.1	86.6	50.0	61.1	65.3	55.5	60.0	65.7
metal nut	60.8	69.0	76.3	54.5	57.4	60.3	63.8	78.2	80.9
pill	35.8	41.7	45.5	33.6	39.0	42.1	44.3	66.7	68.6
screw	38.8	41.5	42.4	26.2	29.4	28.0	57.6	73.4	74.4
tile	85.2	94.5	96.7	68.9	76.3	84.0	79.4	83.0	91.2
transistor	65.6	78.8	78.6	66.1	71.4	83.0	67.8	79.3	88.0
wood	67.5	77.7	86.8	30.9	42.4	36.0	37.1	51.2	45.3
zipper	58.0	67.8	68.2	30.1	38.0	43.6	32.4	45.3	53.8
average	57.9	65.5	68.9	44.2	54.2	57.6	55.0	65.9	69.9

However, the segmentation is not very precious and the masked images still have some normal regions. Hence, we test the images masked by manually annotation (ground-truth), of which the accuracy is further improved.

However, the masked images will still introduce irrelative information, i.e., the white backgrounds. We add a all-white support image as the an ablation class (in the right of Figure 2). The confusion matrix shows that all the query samples are predicted as the most similar to the all-white image.

In summary, there are two major problems in the method that simply combines anomaly segmentation and few-shot learning:

- Anomaly segmentation is not precious, which leads to the gap between manually annotated anomaly area (ground truth).
- The features of masked images are extracted by pertained networks, and the representations of the last layer are used. These embeddings represent the features of the whole masked images, not the critical anomaly regions, which introduces irrelative information.

This inspires us to propose PatchCore, which uses the only features of anomaly regions to calculate the prototypes.

Besides, Table 2 reports the few-shot classification accuracy on different subsets. PatchProto networks achieve great improvement in most of the subsets, while “bottle”, “grid”, “pill” and “transistor” are exceptions. The anomaly in these subsets takes up more image

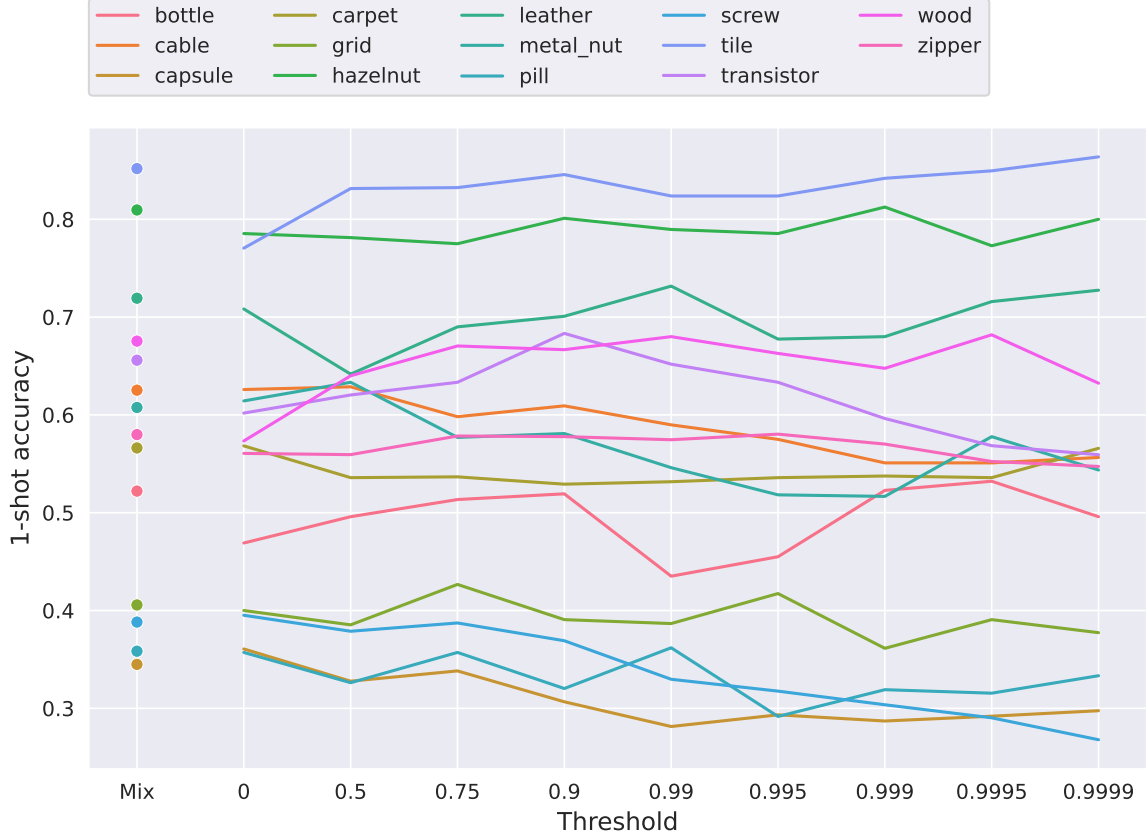


Figure 3: 1-shot classification accuracy under different threshold values.

regions, so the methods take the whole image as the input will perform better. PatchProto networks tend to focus on the most anomaly images region and ignore some global anomaly features, which causes the undesirable performance.

4.4. Parameters

The most critical parameters of PatchProto networks are thresholds to select the anomaly features, i.e., γ in Algorithm 2. Figure 3 shows the 1-shot accuracy of PatchProto networks under different γ values. Larger γ represents that more anomaly regions are selected, while smaller γ represents only the most anomaly regions are used (0 denotes selecting only one patch with highest anomaly score).

We find that high γ value benefits the accuracy of subsets that are easy to classify, i.e., “tile” and “leather”, but some hard-classified subsets like “capsule” and “screw” achieve best performance with single anomaly patch. This is because that hard-classified subsets are also hard to segmentation and anomaly scores on them are inaccurate. The high thresholds will select large image regions, introducing irrelative information. This inspires us to set a upper bound for the number of selected anomaly features, i.e., m in Algorithm 2.

Shown in Figure 3, this mix strategy for anomaly feature selection improves the overall accuracy.

5. Conclusions

This paper propose a few-shot learning method, PatchProto networks, for a practical issue that anomaly samples for training are extremely scarce. PatchProto networks are inspired by PatchCore for anomaly segmentation and Prototype networks for few-shot learning. Nevertheless, unlike classical FSL methods, PatchProto networks fully utilize the normal samples, and only extract CNN features of defective regions of interest, which serves as the prototypes for few-shot learning. The experiment results on MVTec-AD dataset show PatchProto networks significantly improve the anomaly classification accuracy under different few-shot settings. Up to now, PatchProto networks uses a simple approach to calculate the similarity between anomaly features of different length. In future, more sophisticated approach, i.e., LSTM networks, can be applied for calculating the prototype similarity.

References

- [1] An, J., Cho, S., 2015. Variational autoencoder based anomaly detection using reconstruction probability. Special lecture on IE 2 (1), 1–18.
- [2] Bergmann, P., Fauser, M., Sattlegger, D., Steger, C., June 2019. Mvtec ad – a comprehensive real-world dataset for unsupervised anomaly detection. In: Proceedings of the IEEE/CVF Conference on Computer Vision and Pattern Recognition (CVPR).
- [3] Chen, W., Liu, Y., Kira, Z., Wang, Y. F., Huang, J., 2019. A closer look at few-shot classification. CoRR abs/1904.04232.
URL <http://arxiv.org/abs/1904.04232>
- [4] Chen, X., Han, Y., Zhang, J., 2023. A zero-/few-shot anomaly classification and segmentation method for cvpr 2023 vand workshop challenge tracks 1&2: 1st place on zero-shot ad and 4th place on few-shot ad. arXiv preprint arXiv:2305.17382.
- [5] Cohen, N., Hoshen, Y., 2020. Sub-image anomaly detection with deep pyramid correspondences. CoRR abs/2005.02357.
URL <https://arxiv.org/abs/2005.02357>
- [6] Deecke, L., Vandermeulen, R., Ruff, L., Mandt, S., Kloft, M., 2019. Image anomaly detection with generative adversarial networks. In: Berlingerio, M., Bonchi, F., Gärtner, T., Hurley, N., Ifrim, G. (Eds.), Machine Learning and Knowledge Discovery in Databases. Springer International Publishing, Cham, pp. 3–17.
- [7] Defard, T., Setkov, A., Loesch, A., Audigier, R., 2021. Padim: A patch distribution modeling framework for anomaly detection and localization. In: Del Bimbo, A., Cucchiara, R., Sclaroff, S., Farinella, G. M., Mei, T., Bertini, M., Escalante, H. J., Vezzani, R. (Eds.), Pattern Recognition. ICPR International Workshops and Challenges. Springer International Publishing, Cham, pp. 475–489.
- [8] Finn, C., Abbeel, P., Levine, S., 2017. Model-agnostic meta-learning for fast adaptation of deep networks. CoRR abs/1703.03400.
URL <http://arxiv.org/abs/1703.03400>
- [9] Hariharan, B., Girshick, R. B., 2016. Low-shot visual object recognition. CoRR abs/1606.02819.
URL <http://arxiv.org/abs/1606.02819>
- [10] Hu, Y., Liu, R., Li, X., Chen, D., Hu, Q., 2022. Task-sequencing meta learning for intelligent few-shot fault diagnosis with limited data. IEEE Transactions on Industrial Informatics 18 (6), 3894–3904.

- [11] Li, C., Li, S., Zhang, A., He, Q., Liao, Z., Hu, J., 2021. Meta-learning for few-shot bearing fault diagnosis under complex working conditions. *Neurocomputing* 439, 197–211.
URL <https://www.sciencedirect.com/science/article/pii/S0925231221001818>
- [12] Ma, X., Wu, J., Xue, S., Yang, J., Zhou, C., Sheng, Q. Z., Xiong, H., Akoglu, L., 2021. A comprehensive survey on graph anomaly detection with deep learning. *IEEE Transactions on Knowledge and Data Engineering*.
- [13] Natarajan, V., Hung, T.-Y., Vaikundam, S., Chia, L.-T., 2017. Convolutional networks for voting-based anomaly classification in metal surface inspection. In: *2017 IEEE International Conference on Industrial Technology (ICIT)*. pp. 986–991.
- [14] Pang, G., Shen, C., Cao, L., Hengel, A. V. D., mar 2021. Deep learning for anomaly detection: A review. *ACM Comput. Surv.* 54 (2).
URL <https://doi.org/10.1145/3439950>
- [15] Roth, K., Pemula, L., Zepeda, J., Schölkopf, B., Brox, T., Gehler, P. V., 2021. Towards total recall in industrial anomaly detection. *CoRR* abs/2106.08265.
URL <https://arxiv.org/abs/2106.08265>
- [16] Rudolph, M., Wandt, B., Rosenhahn, B., January 2021. Same same but different: Semi-supervised defect detection with normalizing flows. In: *Proceedings of the IEEE/CVF Winter Conference on Applications of Computer Vision (WACV)*. pp. 1907–1916.
- [17] Santos, J., Tran, T., Rippel, O., 2023. Optimizing patchcore for few/many-shot anomaly detection.
- [18] Shi, Y., Yang, J., Qi, Z., 2021. Unsupervised anomaly segmentation via deep feature reconstruction. *Neurocomputing* 424, 9–22.
URL <https://www.sciencedirect.com/science/article/pii/S0925231220317951>
- [19] Simon, A., 2023. Omniglot - writing systems and languages of the world. 25th September 2023. www.omniglot.com.
- [20] Snell, J., Swersky, K., Zemel, R. S., 2017. Prototypical networks for few-shot learning. *CoRR* abs/1703.05175.
URL <http://arxiv.org/abs/1703.05175>
- [21] Vinyals, O., Blundell, C., Lillicrap, T. P., Kavukcuoglu, K., Wierstra, D., 2016. Matching networks for one shot learning. *CoRR* abs/1606.04080.
URL <http://arxiv.org/abs/1606.04080>
- [22] Wah, C., Branson, S., Welinder, P., Perona, P., Belongie, S., 2011. The caltech-ucsd birds-200-2011 dataset. *california institute of technology*.
- [23] Wang, Y., Chao, W., Weinberger, K. Q., van der Maaten, L., 2019. Simpleshot: Revisiting nearest-neighbor classification for few-shot learning. *CoRR* abs/1911.04623.
URL <http://arxiv.org/abs/1911.04623>
- [24] Yi, J., Yoon, S., November 2020. Patch svdd: Patch-level svdd for anomaly detection and segmentation. In: *Proceedings of the Asian Conference on Computer Vision (ACCV)*.
- [25] Zhou, C., Paffenroth, R. C., 2017. Anomaly detection with robust deep autoencoders. In: *Proceedings of the 23rd ACM SIGKDD International Conference on Knowledge Discovery and Data Mining. KDD '17*. Association for Computing Machinery, New York, NY, USA, p. 665–674.
URL <https://doi.org/10.1145/3097983.3098052>
- [26] Zhuo, Y., Ge, Z., 2021. Auxiliary information-guided industrial data augmentation for any-shot fault learning and diagnosis. *IEEE Transactions on Industrial Informatics* 17 (11), 7535–7545.